We are IntechOpen, the world's leading publisher of Open Access books Built by scientists, for scientists

4,800
Open access books available

122,000
International authors and editors

135M
Downloads

Our authors are among the

154
Countries delivered to

TOP 1%
most cited scientists

12.2%
Contributors from top 500 universities

CLARIVATE ANALYTICS BOOK CITATION INDEX INDEXED

WEB OF SCIENCE™

Selection of our books indexed in the Book Citation Index in Web of Science™ Core Collection (BKCI)

Interested in publishing with us?
Contact book.department@intechopen.com

Numbers displayed above are based on latest data collected.
For more information visit www.intechopen.com

9

Improvement of Force Control in Robotic Manipulators Using Sensor Fusion Techniques

J. Gamez[1], A. Robertsson[2], J. Gomez Ortega[1] and R. Johansson[2]
[1]*System Engineering and Automation Department at Jaén University,*
[2]*Automatic Control Department at Lund University*
[1]*Spain,* [2]*Sweden*

1. Introduction

In the never-ending effort of the humanity to simplify their existence, the introduction of 'intelligent' resources was inevitable to come (IFR, 2001). One characteristic of these 'intelligent' systems is their ability to adapt themselves to the variations in the outside environment as the internal changes occurring within the system. Thus, the robustness of an 'intelligent' system can be measured in terms of the sensitivity and adaptability to such internal and external variations.

In this sense, robot manipulators could be considered as 'intelligent' systems; but for a robotic manipulator without sensors explicitly measuring positions or contact forces acting at the end-effector, the robot TCP has to follow a path in its workspace without regard to any feedback other than its joints shaft encoders or resolvers. This restrictive fact imposes severe limitations on certain tasks where an interaction between the robot and the environment is needed. However, with the help of sensors, a robot can exhibit an adaptive behaviour (Harashima and Dote, 1990), the robot being able to deal flexibly with changes in its environment and to execute complicated skilled tasks.

On the other hand, the manipulation can be controlled only after the interaction forces are managed properly. That is why force control is required in manipulation robotics. For the force control to be implemented, information regarding forces at the contact point has to be fed back to the controller and force/torque (F/T) sensors can deliver that information. But an important problem arises when we have only a force sensor. That is a dynamic problem: in the dynamic situation, not only the interaction forces and moments at the contact point but also the inertial forces of the tool mass are measured by the wrist force sensor (Gamez et al., 2008b). In addition, the magnitude of these dynamics forces cannot be ignored when large accelerations and fast motions are considered (Khatib, 1987). Since the inertial forces are perturbation forces to be measured or estimated in the robot manipulation, we need to process the force sensor signal in order to extract the contact force exerted by the robot.

Previous results, related to contact force estimation, can be found in (Uchiyama, 1979), (Uchiyama and Kitagaki, 1989) and (Lin, 1997). In all the cases, the dynamic information of the tool was considered but some of the involved variables, such as the acceleration of the tool, were simply estimated by means of the kinematic model of the manipulator. However, these estimations did not reflect the real acceleration of the tool and thus high accuracy

could not be expected, leading to poor experimental results. Kumar et al. (Kumar and Garg, 2004) applied the same optimal filter approach to multiple cooperative robots.
Later, in (Gamez et al., 2004), (Gamez et al., 2005b), (Gamez et al., 2006b) and (Gamez et al., 2007b), Gamez et al. presented a contact force estimator restricting initially the results to one and three dimensions. In these works, they proposed a new contact force estimator that fused the information of a wrist force sensor, an accelerometer placed at the robot tool and the joint position measurements, in order to differentiate the contact force measurements from the wrist force sensor signals. They proposed combining the F/T estimates from model based observers with F/T and acceleration sensor measurements in tasks with heavy tools interacting with the environment. Many experiments were carried out on different industrial platforms showing the noise-response properties of the model-based observer validating its behaviour. For these observers, self-calibrating algorithms were proposed to easily implement them in industrial robotic platforms (Gamez et al., 2008a); (Gamez et al., 2005a).
In addition, Kröger et al. (Kröger et al., 2006); (Kröger et al., 2007) also presented a contact F/T estimator based on this sensor fusion approach. In this work, they presented a contact F/T estimator based also on the integration of F/T and inertial sensors but they did not consider the stochastic properties of the system. Finally, a 6D contact force/torque estimator for robotic manipulators with filtering properties was recently proposed in (Gamez et al., 2008b).
This work describes how the force control performance in robotic manipulators can be increased using sensor fusion techniques. In particular, a new sensor fusion approach applied to the problem of the contact force estimation in robot manipulators is proposed to improve the manipulator-environment interaction. The presented strategy is based on the application of sensor fusion techniques that integrate information from three different sensors: a wrist force/torque (F/T) sensor, an inertial sensor attached to the end effector, and joint sensors. To experimentally evaluate the improvement obtained with this new estimator, the proposed methodology was applied to several industrial manipulators with fully open software architecture. Furthermore, two different force control laws were utilized: impedance control and hybrid control.

2. Problem Formulation

Whereas force sensors may be used to achieve force control, they may have drawbacks if used in harsh environments and their measurements are complex in the sense that they reflect forces other than contact forces. Furthermore, if the manipulator is working with heavy tools interacting with the environment, the magnitude of these dynamics forces cannot be ignored, forcing control engineers to consider some kind of compensator that eliminates the undesired measurements. In addition, these perturbations, particulary the inertial forces, are higher when large accelerations and fast motions are considered.
In this context, let us consider a robot manipulator where a force sensor has been placed at the robot wrist and that an inertial sensor has been attached to the robot tool to measure its linear acceleration and angular velocity (Fig. 1). Then, when the robot manipulator moves in either free or constrained space, a F/T sensor attached to the robot tip measures not only the contact forces and torques exerted to the environment but also the non-contact ones produced by the inertial and gravitational effects. That is,

$$\begin{pmatrix} \vec{F}_S \\ \vec{N}_S \end{pmatrix} = \begin{pmatrix} \vec{F}_E \\ \vec{N}_E \end{pmatrix} + \begin{pmatrix} \vec{F}_I \\ \vec{N}_I \end{pmatrix} + \begin{pmatrix} \vec{F}_G \\ \vec{N}_G \end{pmatrix} \quad (1)$$

where $\vec{F}_S$ and $\vec{N}_S$ are the forces and torques measured by the wrist sensor; $\vec{F}_E$ and $\vec{N}_E$ are the environmental forces and torques; $\vec{F}_I$ and $\vec{N}_I$ correspond to the inertial forces and torques produced by the tool dynamic and $\vec{F}_G$ and $\vec{N}_G$ are the forces and torques due to gravity. Normally, the task undertaken requires the control of the environmental force $\vec{F}_E$ and the torque $\vec{N}_E$.

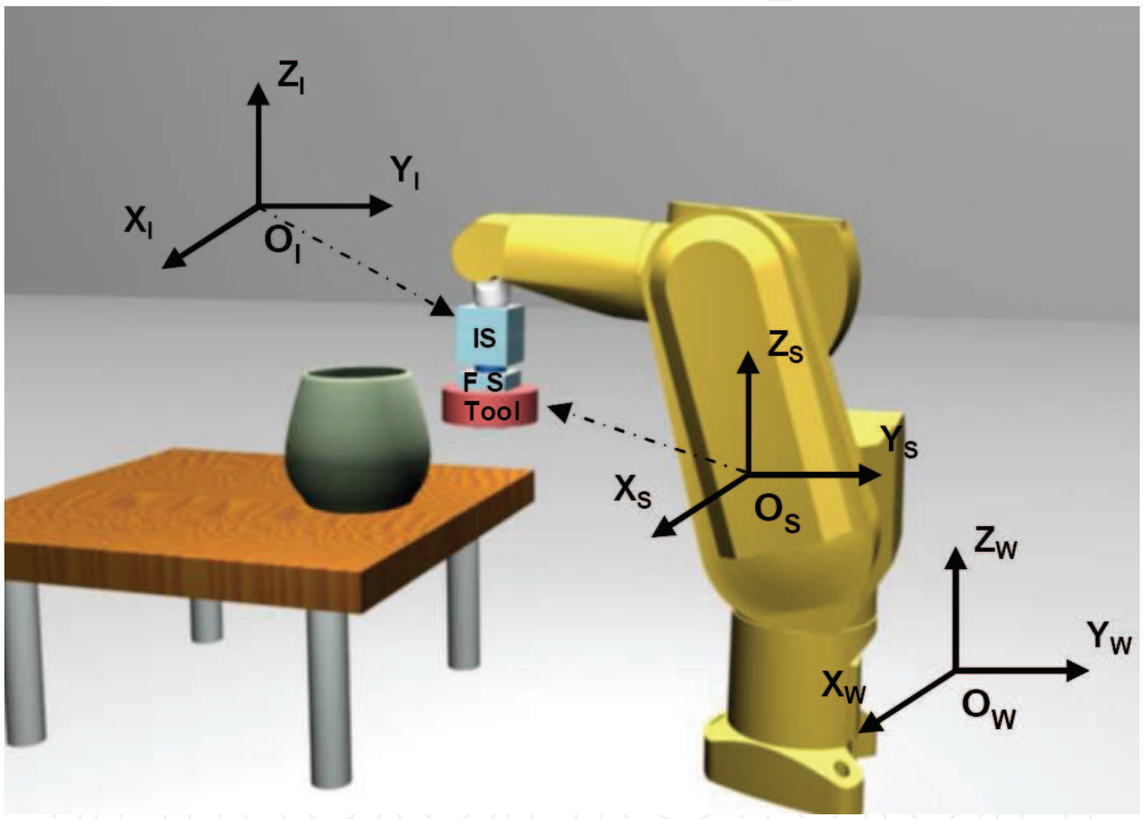

Figure 1. Coordinate frames of the robotic system. The sensor frames of the robot arm ($\{O_W X_W Y_W Z_W\}$), of the force-torque sensor (FS) ($\{O_S X_S Y_S Z_S\}$) and of the inertial sensor (IS) ($\{O_I X_I Y_I Z_I\}$) are shown

The main goal of this work is to evaluate how the implementation of a contact force/torque estimator, that distinguishes the contact F/T from the wrist force sensor measurement, can improve the force control loop in robotic manipulators. This improvement has to be based in the elimination of the non-desired effects of the non-contact forces and torques and, moreover, to the reduction of the high amount of noise introduced by some of the sensors used.

3. 6DOF Contact Force-Torque Estimator

3.1 Description of Coordinate Frames and Motion

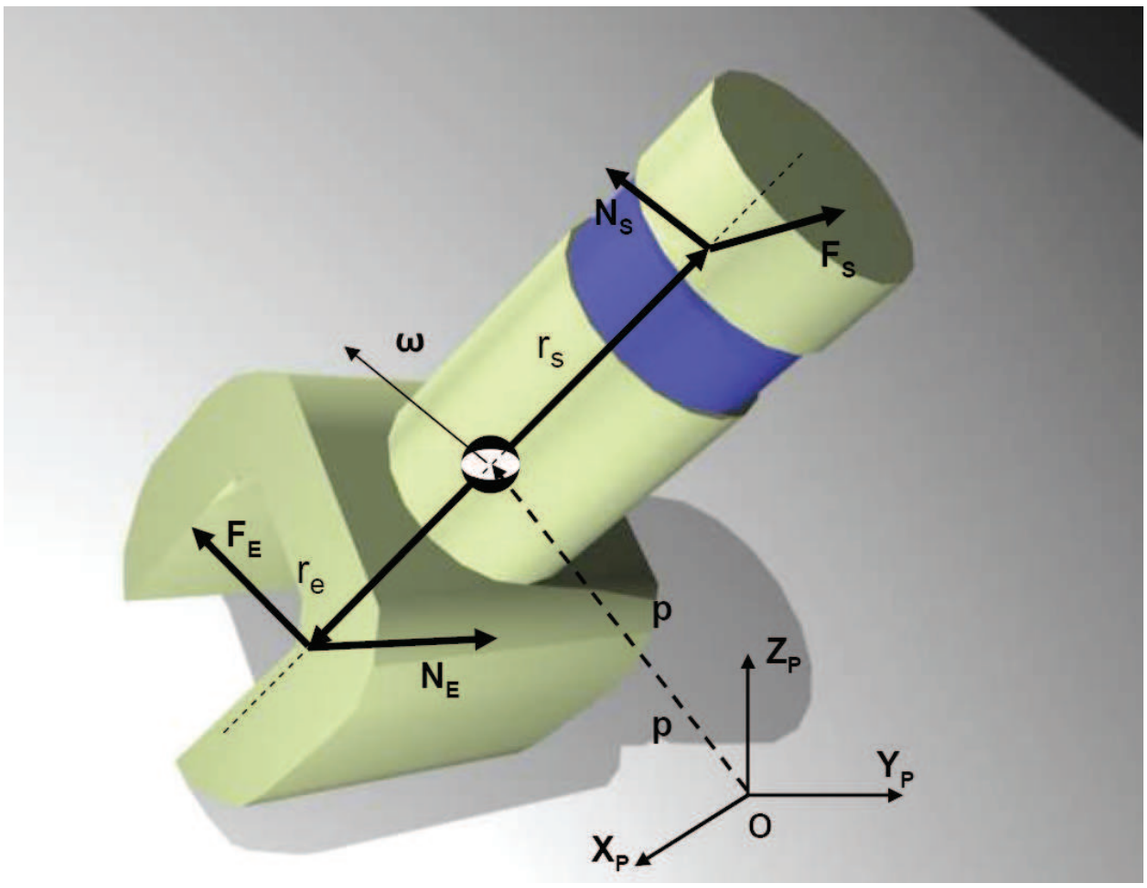

Figure 2. Force and moments applied to the robot tool

As shown in Fig. 1, let us consider an inertial sensor attached to the robot tool. Then, $\{O_S X_S Y_S Z_S\}$ and $\{O_I X_I Y_I Z_I\}$ correspond to the force sensor and the inertial sensor frames respectively. The world frame is an inertial coordinate system represented by $\{O_W X_W Y_W Z_W\}$ and without loss of generality we let it coincide with the robot frame for simplified notation. Let $\{{}^W R_S\}$ and $\{{}^S R_I\}$ denote the rotation matrices that relate the force sensor to the world frames and the inertial sensor to the force sensor frames, respectively. Assume that the force sensor is rigidly attached to the robot tip and that the inertial sensor can be placed either in the tool or at the robot wrist.

Let us also define the following frames to characterize the robot tool or end effector (Fig. 2): $\{O_E X_E Y_E Z_E\}$ is the end effector coordinate system by which the components of the external force and moment are represented and $\{O_P X_P Y_P Z_P\}$ represents the coordinate system fixed to the end effector so that $\{O_P\}$ coincides with the center of gravity and the $\{X_P\}$, $\{Y_P\}$, and $\{Z_P\}$ axes with the principal axes of the end effector.

3.2 Force-Torque Transformation

The set of forces F ($F \in \mathbb{R}^3$) and moments N ($N \in \mathbb{R}^3$) referred to frame A can be defined using *wrench* notation (Murray et al, 1994) as :

$$ {}^{A}U_{A} = \begin{pmatrix} {}^{A}F_{A} \\ {}^{A}N_{A} \end{pmatrix} \tag{2} $$

which can be transformed into a new frame B applying the following transformation

$$ \begin{pmatrix} {}^{B}F_{A} \\ {}^{B}N_{A} \end{pmatrix} = \begin{pmatrix} {}^{B}R_{A}^{T} & 0_{3\times3} \\ -{}^{B}R_{A}^{T\,B}p^{x} & {}^{B}R_{A}^{T} \end{pmatrix} \begin{pmatrix} {}^{A}F_{A} \\ {}^{A}N_{A} \end{pmatrix} \tag{3} $$

where ${}^{B}R_{A}$ is the rotation matrix that relates frame A to frame B, and matrix ${}^{B}p^{x}$ is obtained as (Murray et al, 1994):

$$ {}^{B}p^{x} \times q = {}^{B}p^{x} q, \qquad {}^{B}p^{x} = \begin{pmatrix} 0 & -p_3 & p_2 \\ p_3 & 0 & -p_1 \\ -p_2 & p_1 & 0 \end{pmatrix} \tag{4} $$

being ${}^{B}p^{x}$ the position vector from $\{O_B\}$ to $\{O_A\}$ with ${}^{B}p^{x}$, $q \in \mathbb{R}^3$.

3.3 Robot Tool Dynamics Modeling

The F/T sensor measures not only the contact forces and torques, but also the disturbances produced by the non-contact forces and torques (inertial and gravitational effects) due to the robot tool dynamics. From Fig. 2, the tool dynamics is modeled using forces and torques that occur between the robot tool and the manipulator tip and that are measured by the wrist F/T sensor ${}^{S}F_{S}$ and ${}^{S}N_{S}$; and, on the other hand, the forces and moments exerted by the manipulator tool to its environment (${}^{E}F_{E}$ and ${}^{E}N_{E}$). Then, from a static equilibrium relation using wrench notation (Murray et al, 1994), the force and moment in $\{O_P\}$ are obtained as:

$$ {}^{P}U_{P} = \begin{pmatrix} {}^{P}F_{P} \\ {}^{P}N_{P} \end{pmatrix} = \begin{pmatrix} {}^{P}R_{S}^{T} & 0_{3\times3} \\ -{}^{P}R_{S}^{T\,S}p^{x} & {}^{P}R_{S}^{T} \end{pmatrix} \begin{pmatrix} {}^{S}F_{S} \\ {}^{S}N_{S} \end{pmatrix} + \begin{pmatrix} {}^{P}R_{E}^{T} & 0_{3\times3} \\ -{}^{P}R_{E}^{T\,E}p^{x} & {}^{P}R_{E}^{T} \end{pmatrix} \begin{pmatrix} {}^{E}F_{E} \\ {}^{E}N_{E} \end{pmatrix} $$

$$ = {}^{P}T_{S} \begin{pmatrix} {}^{S}F_{S} \\ {}^{S}N_{S} \end{pmatrix} + {}^{P}T_{E} \begin{pmatrix} {}^{E}F_{E} \\ {}^{E}N_{E} \end{pmatrix} \tag{5} $$

with ${}^{P}R_{S}$, ${}^{P}R_{E}$ being the rotation matrices that relate frames $\{S\}$ and $\{E\}$ to frame $\{P\}$; ${}^{S}p^{x}$ and ${}^{E}p^{x}$ are matrices of dimension 3×3 obtained from Eq. (4) where p is the position

vector from $\{O_P\}$ to $\{O_S\}$ or from $\{O_P\}$ to $\{O_E\}$. Finally, applying the Newton-Euler equations, the dynamics of the robot tool are defined as

$$
{}^{P}U_{P} = \begin{pmatrix} m^{W}R_{P}^{-1\,W}R_{I}\,a - m^{W}R_{P}^{-1}g \\ \mathcal{I}^{P}R_{I}\dot{\omega} + {}^{P}R_{I}\omega \times \mathcal{I}^{P}R_{I}\omega \end{pmatrix}
$$

$$
= \begin{pmatrix} m^{W}R_{P}^{-1W}R_{I} & 0_{3x3} \\ 0_{3\times3} & \mathcal{I}^{P}R_{I} \end{pmatrix} \begin{pmatrix} a \\ \dot{\omega} \end{pmatrix} + \begin{pmatrix} -m^{W}R_{P}^{-1} & 0_{3\times3} \\ 0_{3\times3} & ({}^{P}R_{I}\omega)^{\times}\mathcal{I}^{P}R_{I} \end{pmatrix} \begin{pmatrix} g \\ \omega \end{pmatrix} \tag{6}
$$

where m is the robot tool mass, $a = [\ddot{x}, \ddot{y}, \ddot{z}]^T$ is the robot tool acceleration measured in the inertial frame $\{I\}$; $g = [g_x, g_y, g_z]^T$ is the gravity acceleration vector; $\omega = [\omega_1, \omega_2, \omega_3]^T$ is the angular velocity of the robot tool with respect to frame $\{I\}$. Matrix $\mathcal{I}$ denotes the moment of inertia of the robot tool calculated with respect to the frame $\{P\}$ (Gamez et al., 2008b).

3.4 Contact Forces and Torques Estimator

The objective of the force observer is to estimate the environmental forces and torques by separating them from the end-effector inertial and gravitational forces and moments in the measurement given by the force sensor. As the sensor fusion approach considered integrates the information from different sensors, which may be quite noisy, it is necessary to consider an estimator with filtering properties.

To define the robot tool dynamics, Eqs. (5-6) are translated to state space formulation. Let then us consider the following state space vector

$$
X = [x, y, z, \theta, \phi, \psi, \dot{x}, \dot{y}, \dot{z}, \omega_1, \omega_2, \omega_3] \tag{7}
$$

where x, y, z are the position coordinates of the robot tool center of mass ($p = (x, y, z)^T$) and θ, ϕ and ψ are the Euler angles that define the robot tool orientation ($o = (\theta, \phi, \psi)^T$). Both refer to the $O_W X_W Y_W Z_W$ frame. $\dot{x}, \dot{y}, \dot{z}$ correspond to the linear velocity of the robot tool center of mass.

Those variables that can be measured are regarded as outputs: the robot tool position and orientation (p, o), the F/T sensor signals (F_s, N_s), the angular velocities (ω) and the robot tool linear acceleration ($\ddot{p}$). (ω) and ($\ddot{p}$) are measured through the inertial sensor. In addition, the angular accelerations $\dot{\omega}$ of the robot tool are estimated using the angular velocities, also including them as outputs. Thus the output vector Y will be :

$$
Y = \left(p^T, o^T, F_s^T, N_s^T, \omega^T, \ddot{p}^T, \dot{\omega}^T \right)^T \tag{8}
$$

Then, we propose the following state space system

$$
\begin{cases} \dot{X} = A(X)X + B_S U_S + B_E U_E + B_G g + \nu_X \\ Y = C(X)X + D_S U_S + D_E U_E + D_G g + \nu_y \end{cases} \tag{9}
$$

where g is the gravity vector, $U_S = [{}^S F_S^T, {}^S N_S^T]^T$, and $U_E = [{}^E F_E^T, {}^E N_E^T]^T$. ν_X and ν_y are, respectively, the process and the output noises. Matrices $A(X)$, B_S, B_E, B_G, $C(X)$, D_S, D_E and D_G obtain their values from Eqs. (5) and (6) (Gamez et al., 2008b).

Note the non-linearity of the system through the entries A_1 and A_2 in the matrices $A(X)$ and $C(X)$.

In this context, an observer where input U_E has not been considered is proposed as (Gamez et al., 2004); (Gamez et al., 2005b):

$$\widehat{X} = A(X)\widehat{X} + B_S U_S + B_G g + L(t)(Y - \hat{Y}) \tag{10}$$

$$\hat{Y} = C(X)\widehat{X} + D_S U_S + D_G g \tag{11}$$

where $\widehat{X}$ corresponds to the state estimation of X and $L(t)$ is the observer gain for a given instant t: Then, the dynamics of the estimation error $\widetilde{X} = X - \widehat{X}$ are obtained as

$$\widetilde{X} = (A(X) - L(t)C(X))\widetilde{X} + (B_E - L(t)D_E)U_E + \nu_X - L(t)\nu_y \tag{12}$$

$$\widetilde{Y} = Y - \hat{Y} = C(X)\widetilde{X} + D_E U_E + \nu_y \tag{13}$$

Then, a dynamic force estimator is defined as:

$$\widehat{U}_E = D_E^{\dagger}(-C(X)\widetilde{X} + \widetilde{Y}) \tag{14}$$

where $D_E^{\dagger}$ is the Moore-Penrose pseudoinverse of D_E (Johansson, 1993).

Note that, from Eqs. (10) and (12), the core of the estimator is to combine F/T estimates from model based observers, where the input U_E has not been considered, with F/T, inertial and position measurements, in order to obtain a dynamic contact F/T estimator with low-pass properties.

3.5 Observer Gain Selection

While there are many application-specific approaches to estimating an unknown state from a set of process measurements, many of these methods do not inherently take into consideration the typically noisy nature of the measurements. In our case, while the contact F/T estimates vary with the robotic task, the fundamental sources of information are always the same: wrist F/T, inertial and position measurements. All of them are derived from noisy sensors. This noise is typically statistical in nature (or can be effectively modeled as such), which leads us to stochastic methods for addressing the problems. The solution adopted for this work is the Extended Kalman Filter (Jazwinski, 1970).

Considering that stochastic disturbances are present in our system (Eq. (9)) and supposing that the process noises ν_X and ν_y are white, Gaussian, zero mean, and independent with

constant covariance matrices Q and R respectively, then, there exists an optimal Extended Kalman Filter gain $L(t)$ for the state space system (12) that minimizes the estimation error variance due to the system noise (Grewal and Andrews, 1993) that, in our case, is directly related to minimizing the variance of the contact F/T estimation error. That is, as the variance of the F/T is not stationary under relevant conditions of application, there is no unique optimal observer gain.
Since matrices $A(X)$ and $C(X)$ from Eqs. (10) and (11) are non-linear, a linearization of the system for an online estimated trajectory $\overline{X}(t)$ is used to select $L(t)$ (see (Gamez et al., 2008b) for more details).

4. Improvement of Force Control in Robotic Manipulators

For the applied force control laws used to fully test the contact force observer, note that the dynamic interaction between a manipulator and an environment occurring during assembly tasks or manufacturing requires frequent exchanges between a free motion and a constrained motion making desirable to have a unified approach to position and force control. That is why all the results are mainly obtained using an impedance control as force control law. However, another different force control law has been used to validate the behavior of the contact force observer: Hybrid position-force control. To analyze the behavior of the force control loops where the force estimator is used, two industrial manipulators were used: an ABB system and a Stäubli manipulator.

4.1 Force control loop utilized

A brief explanation of the implemented control laws is developed as follows.

4.1.1 Impedance Control

Since the proposed observer must work in both free space and constrained space, it is interesting to use a force control law which allows a manipulator to handle both types of motion without switching control strategies during transitions. In this sense, the impedance control (Hogan, 1985) manages how stiff the end-point comes into contact with the environment and required no control mode switching. However, it can not command the contact forces directly. The motivation of the impedance control is that, instead of controlling position and force separately in task space, the desirable dynamic behavior of a manipulator is specified as a relation between force and motion, referred to as impedance, and accomplished based on an estimated or sensed contact force.
As pointed out in (Hogan, 1985), the environmental model is central to any force strategy. Basically, a second-order mass-spring-damper system is used to specify the target dynamics. However simpler models such as pure stiffness or combination of dampening and stiffness can also be used (Whitney, 1985). In this manner, the equation of the dynamic relationship between the end-effector position $\vec{p} = [x, y, z]$ and the contact force $\vec{F}_E$ used to control the force exerted to the environment is

$$\vec{F}_E = B(\dot{\vec{p}}_r - \dot{\vec{p}}) + K(\vec{p}_r - \vec{p}) \tag{15}$$

where the diagonal matrices B and K contain the impedance parameters along Cartesian axes representing the damping and stiffness of the robot respectively, $\vec{p}$ is the steady state nominal equilibrium position of the end effector in the absence of any external forces and $\vec{p}_r$ is the reference position. As $\vec{p}_r$ is software specified, it may reach positions beyond the reachable workspace or inside the environment during contact with the environment. Note that for a desired static behavior of the interaction, the impedance control is reduced to a stiffness control (Chiaverini et al., 1999).
To carry out the impedance control, a LQR controller was used to make the impedance relation variable go to zero for the three axes (x, y, z) (Johansson and Robertsson, 2003). The control law applied was

$$u = -L \cdot \vec{p} + f \cdot \hat{\vec{F}}_E + l_r \vec{p}_r \tag{16}$$

with f as the force gains in the impedance control, $\hat{\vec{F}}_E$ the estimated environmental force, which, in our case, was estimated using the contact force observer, $\vec{p}_r$ the position reference and l_r the position gain constants, L being calculated considering the linear model of the robot system.

4.1.2 Hybrid Control

Consider the contact force $\vec{F}_E$ and the end-effector position $\vec{p}$, expressed in the world frame $O_W X_W Y_W Z_W$, which are estimated through the force observer and measured through the joint sensors and the kinematic model respectively. Denoting the desired values for $\vec{F}_E$ and $\vec{p}$ as $\vec{F}_E^d$ and $\vec{p}^d$, respectively, we obtain expressions for the position and force errors after considering their directions to be controlled:

$$\vec{p}^e = (I - S)[\vec{p}^d - \vec{p}] \tag{17}$$

$$\vec{F}_E^e = (S)[\vec{F}_E^d - \vec{F}_E] \tag{18}$$

where I is the unity matrix and S is the selection matrix for the force controlled directions. Using Eqs. (17) and (18), a hybrid control law can be given by:

$$\tau(t) = \tau_P(t) + \tau_F(t) \tag{19}$$

$$\tau_P(t) = K_{P_p} \vec{p}^e + K_{P_d} \dot{\vec{p}}^e \tag{20}$$

$$\tau_F(t) = K_{F_i} \int_0^t \vec{F}_E^e dt \tag{21}$$

where $\tau_P(t)$ compensates for the position error and $\tau_F(t)$ compensates for the force error. Applying this control law one can expect that the component of the desired position $\vec{p}^d$ and the component of the desired force $\vec{F}_c^d$ are closely tracked.

4.2 Experimental Platforms

Two different platforms were used to validate the behavior of the resulting contact force observers. The first one, placed in the Robotics Lab at the Department of Automatic Control, Lund University, is composed of the following devices and sensors (Fig. 3): an ABB IRB 2400 robot, a JR3 wrist force sensor, a compliant grinding tool that links the robot tip and the tool, and a capacitive 3D accelerometer.

This platform was based on an ABB robot. A totally open architecture is its main characteristic, permitting the implementation and evaluation of advanced control strategies. The controller was implemented in Matlab/Simulink using the Real Time Workshop of Matlab, and later compiled and linked to the Open Robot Control System (Nilsson and Johansson, 1999); (Blomdell et al., 2005). The wrist sensor used was a DSP-based force/torque sensor of six degrees of freedom from JR3. The tool used for our experiments was a grinding tool with a weight of 12 kg. The mechanical device Optidrive-in itself a linear force sensor-the purpose of which was to provide to the tool additional compliance in the contact with the environment, was considered as a spring-damping system and provided a measure of the force exerted between its extremes. The accelerometers were placed on the tip of the tool to measure its acceleration. The accelerometer and Optidrive signals were read by the robot controller in real time via analog inputs.

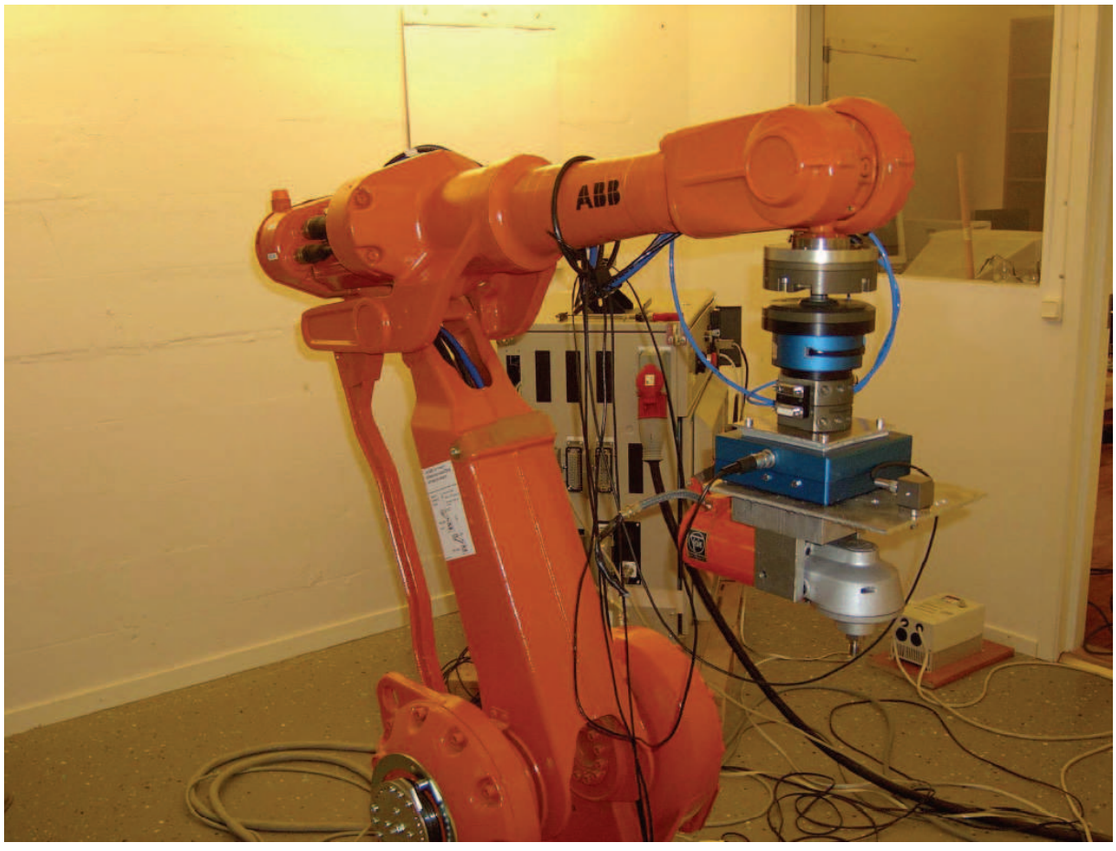

Figure 3. The ABB experimental setup. An ABB industrial robot IRB 2400 with an open control architecture system is used. The wrist sensor is placed between the robot TCP and a compliance tool where the grinding tool is attached. The accelerometer is placed on the tip of the grinding tool

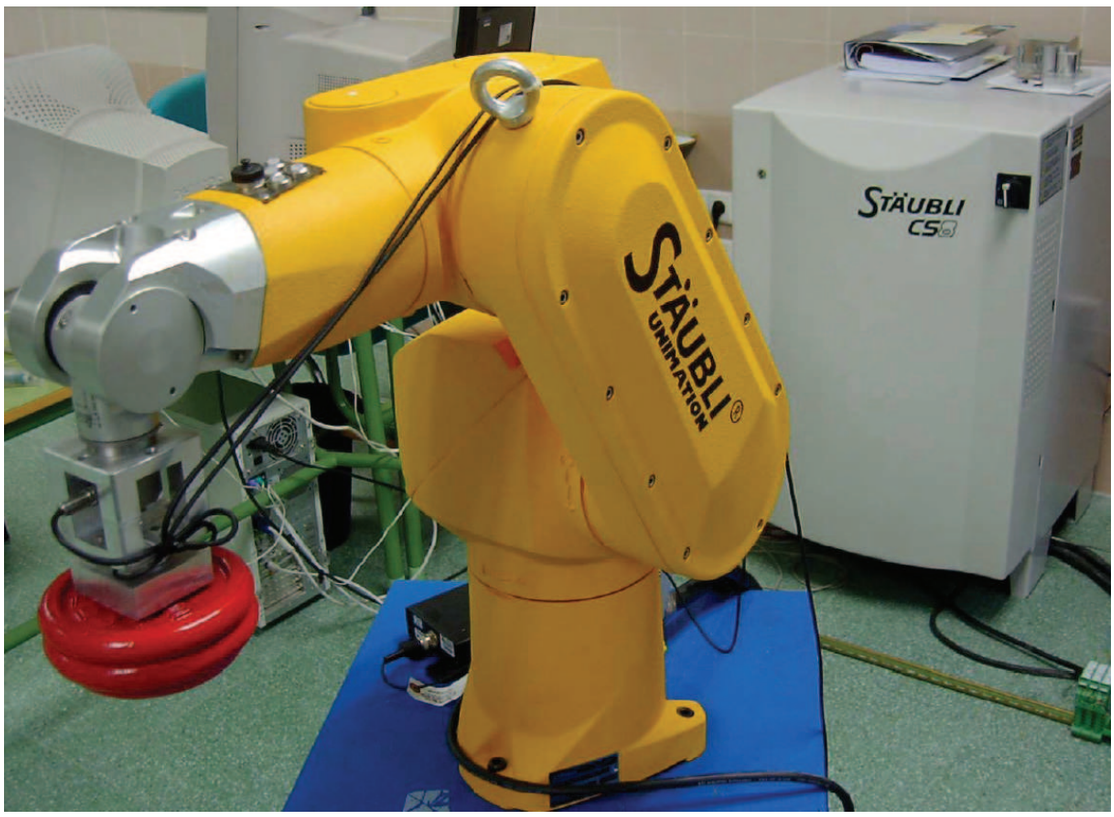

Figure 4. Stäubli Platform. An RX60 robot with an open control architecture system is used. An ATI wrist force sensor is attached to the robot tip. The accelerometer is placed between the robot TCP and the force sensor

Regarding the second robotic platform (Fig. 4), it consisted of a Stäubli manipulator situated in the Robotics and Automation Lab at Jaen University, Spain. It is based on a RX60 which has been adapted in order to obtain a completely open platform (Gamez et al., 2007a). This platform allows the implementation of complex algorithms in Matlab/Simulink where, once they have been designed, they were compiled using the Real Time Toolbox and downloaded to the robot controller. The task created by Simulink communicates with other tasks through shared memory. Note that the operative system that managed the robot controller PC is VxWorks (Wind River, 2005).
For the environment, in both situations a vertical screen made of cardboard, whose stiffness was determined experimentally, was used to represent the physical constraint.
With regard to the sensors, an ATI wrist force sensor together with an accelerometer was attached to the robot flange. Both sensors were read via analog inputs (Gamez et al., 2003). The acceleration sensor is a capacitive PCB sensor with a real bandwidth of 0-250Hz.

4.3 Experimental Results

In this subsection, the results obtained from the contact force observers to both robotic platforms are described. Firstly, the results obtained applying the estimator to the Stäubli platform are presented in Fig. 5. The first experiment consisted of a linear movement in the axis z of three phases: an initial movement in free space (from t =5s to t = 6.2s), a contact

transition (from t =6.2s to t = 6.4s) and a movement in constrained space (from t =6.4s to t = 9s). The force controller was an impedance one. In this case, it can be compared how the observer eliminates the inertial effects and the noise introduced by the sensors. Regarding the noise spectra, in Fig. 6, the power spectrum density for the composed signal $u - m\ddot{\xi}_z$ (left) and the observer output power spectrum density (right) are shown. Note how the observer cuts off the noise introduced by the sensors.

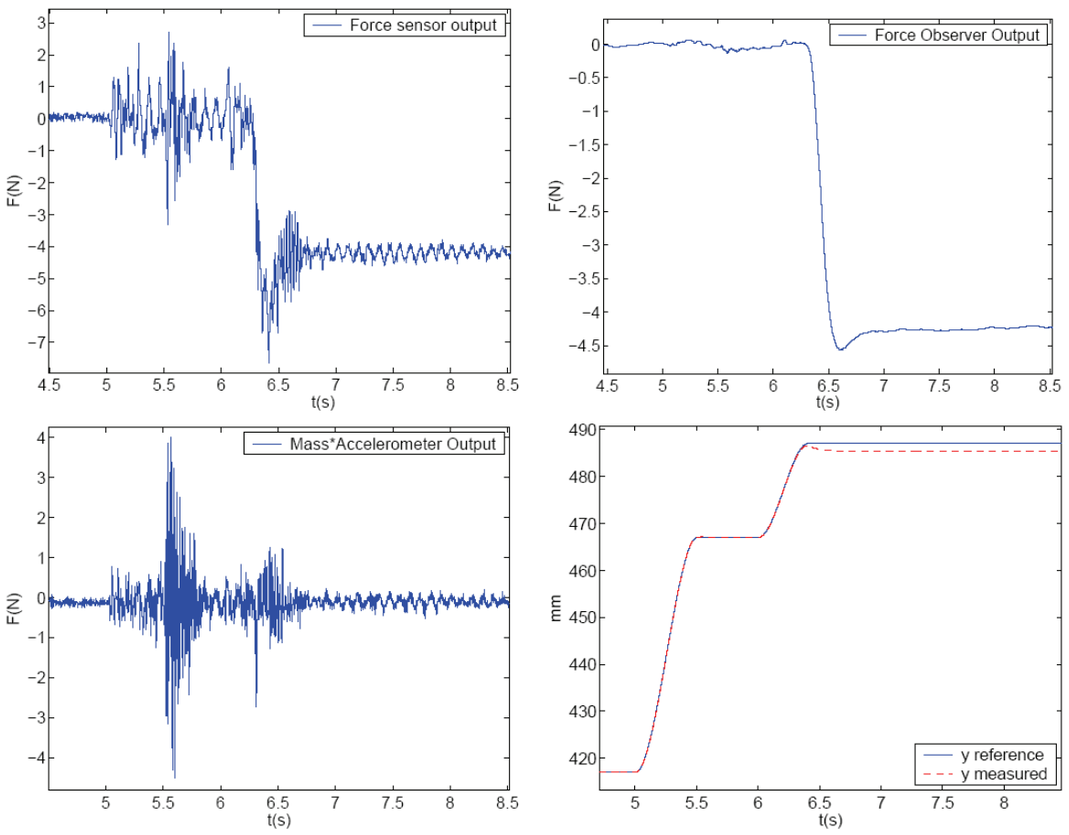

Figure 5. Force measurement from the wrist sensor ATI (upper-left), force observer output (upper-right), accelerometer output (lower-left) and real and measured position of the robot tip for y-axis (lower-right)

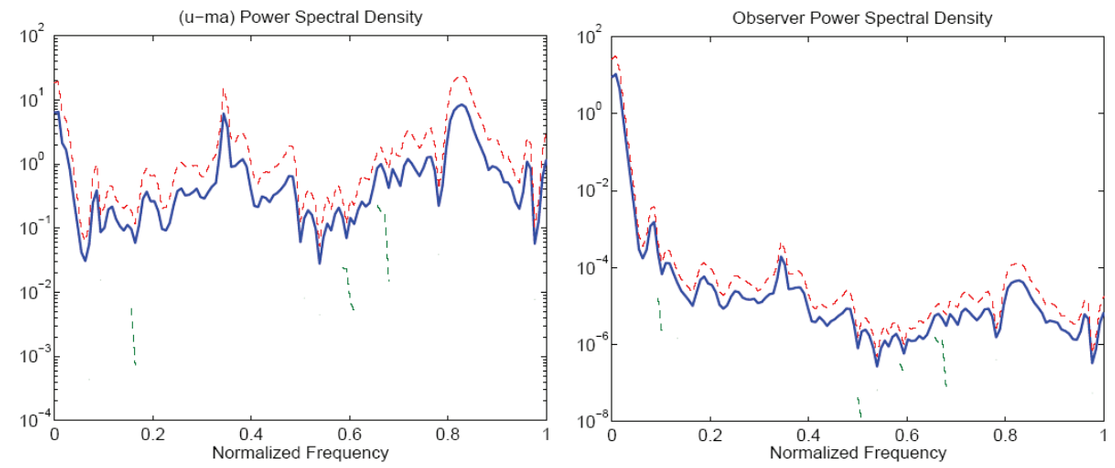

Figure 6. Power spectrum density for the composed signal $u - m\ddot{z}$ (left) and observer output power spectrum density (right). The sample frequency is 250 Hz

On the other hand, another experiment was executed consisting of an oscillation movement for one of the Cartesian axis. Results are depicted in Fig. 7. From this figure it can be verified how the observer eliminates the force oscillations due to the inertial forces that are measured by the force sensor. Note that the movement follows a cubic spline, which means that the acceleration is almost a straight line.

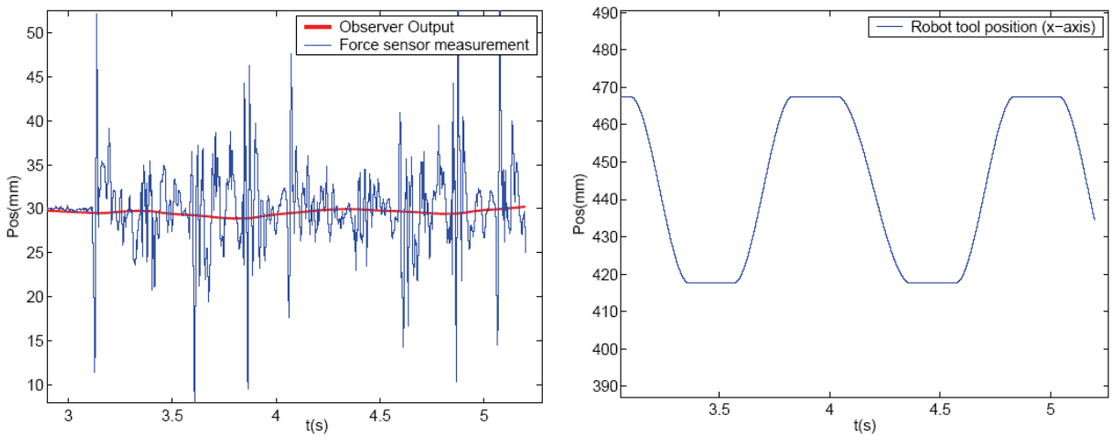

Figure 7. Force sensor measurement and Observer output (left) and robot tool position (right) measured during an oscillation movement in free space

Another experiment carried out consisted of the same former phases but the force control loop is a hybrid control one. In Fig. 8, the ATI force sensor measurement and the observer output are shown. From this figure it is possible to verify how the observer eliminates the force oscillations due to the inertial forces at the beginning of the experiment (where the robot is moving in free space).

Regarding the experiments carried out on the ABB robot, they consisted of three phases for all axes (x, y, z) as well: an initial movement in free space, a contact transition and later, a movement in constrained space. The velocity during the free movement was 300 mm/s and the angle of impact was 30 degrees with respect to the normal of the environment.

The experiments for axis x are shown in Fig. 9, which depicts, at the top, the force measurement from the ATI sensor (left) and the force observer output (right) while at the bottom, the acceleration of the tool getting into contact with the environment (left), and the observer compensation (right). Note that the observer eliminates the inertial effects.

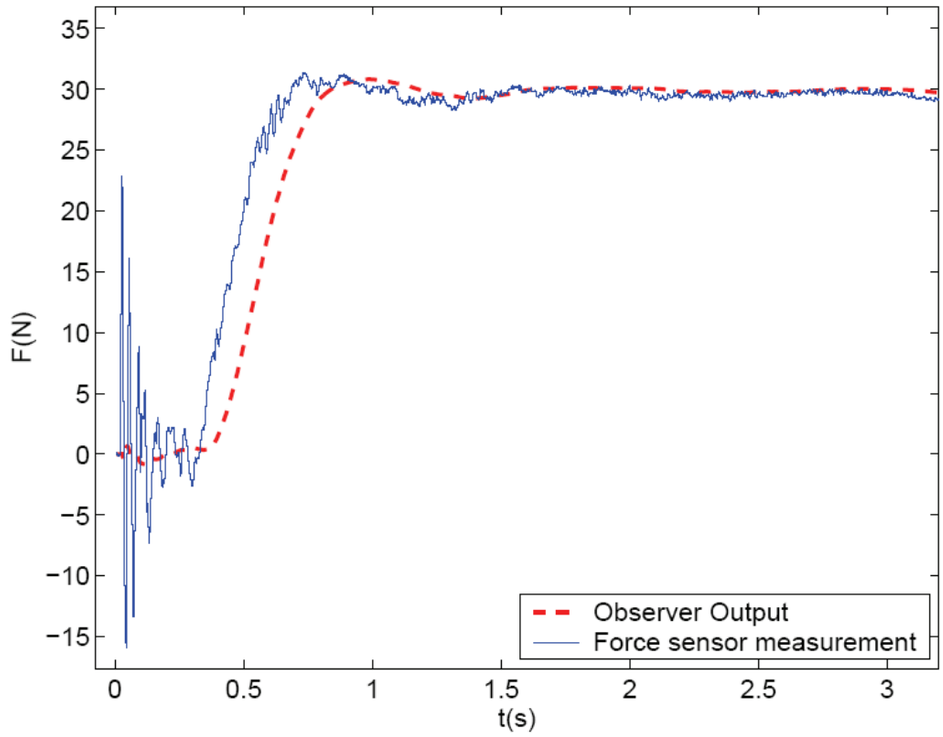

Figure 8. Force sensor and observer output in a hybrid force/position control loop

To test the torque estimation effects, Fig. 10 shows an experiment where, first the robot tool followed an angular trajectory in free space varying the Euler angle ϕ and, later, the manipulator gets into contact with the environment. Fig. 10 (a) and (b) show how the inertial disturbances can be indirectly measured through the angular velocity sensor. Fig. 10 (c) depicts a comparison between the torque sensor measurement N_{S_y} and the contact torque estimator N_{E_y}. It can be observed how the estimator eliminates the disturbances produced by the inertial torques due to the robot tool angular velocity. Fig. 10 (d), (e) and (f) show the power spectrum density of the torque measurement, the angular velocity measurement and the contact torque estimator, respectively. In these spectra, the dynamic filtering properties of the proposed estimator can be noted since the proposed observer

filters the noise introduce mainly by the torque sensor at 0.15 of the normalized frequency.

Another strategy could be that, starting from the premise we have attached an accelerometer to the robot tool to determine the tool acceleration, why not to to subtract the tool acceleration multiplied by the tool mass from the force sensor measurement. However, as both the accelerometer and the force sensors are quite noisy elements, it must be pointed out that we would have a final signal with too much noise with simple addition of accelerometer sensors. Then, a next step to be applied is, after subtracting from the force sensor measurement the tool acceleration pondered by the tool mass, why not to apply a standard low-pass filter to eliminate the noise introduced by the sensors. To this purpose, we compare the performance of the proposed force observer against different standard low-pass filters in order to validate the proposed contact force estimator. The most common types of low-pass filters-i.e. Butterworth filter, Chebyshev filters (type I and II) and, finally, an elliptic filter-will be compared using the ABB platform as benchmark.

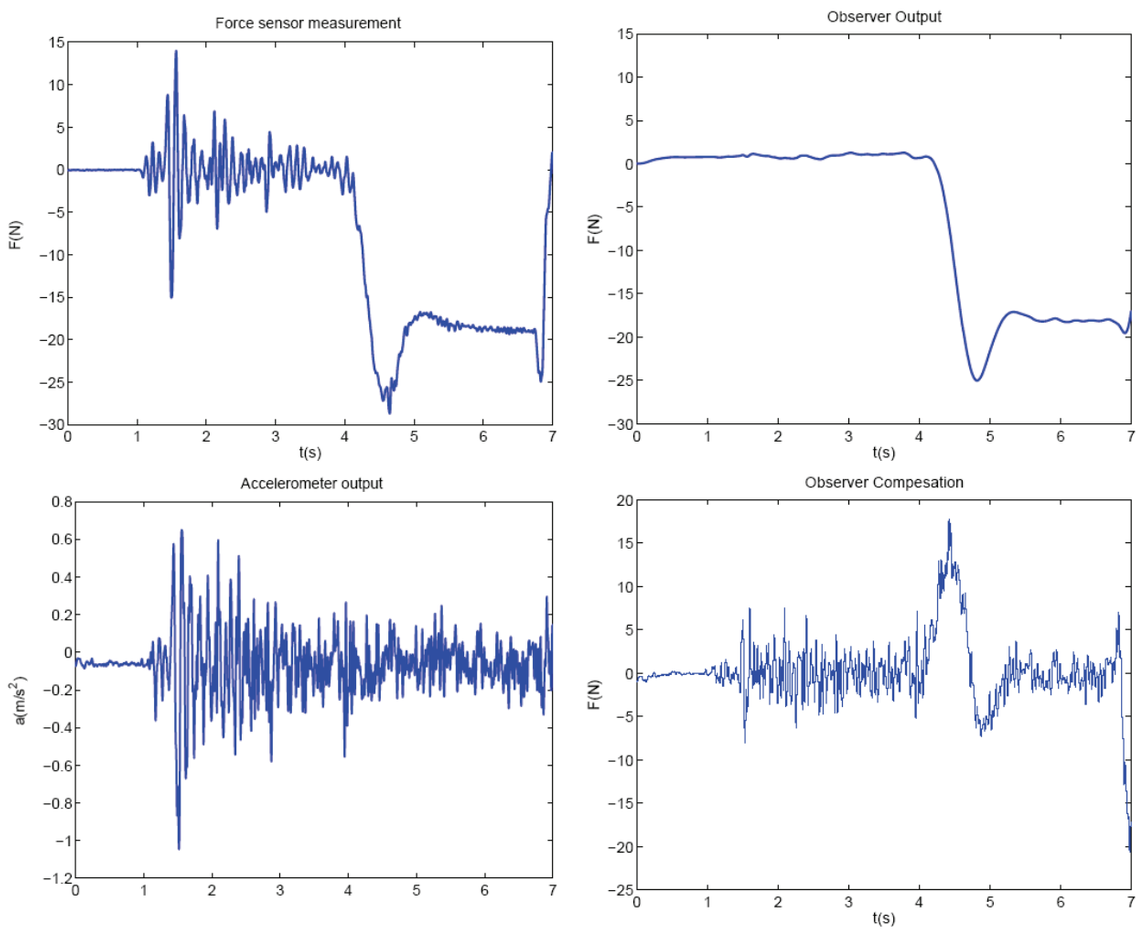

Figure 9. Force measurement from the wrist sensor (upper-left), force observer output (upper-right), acceleration of the robot TCP (lower-left) and observer compensation (lower-right). These results were obtained for x-axis

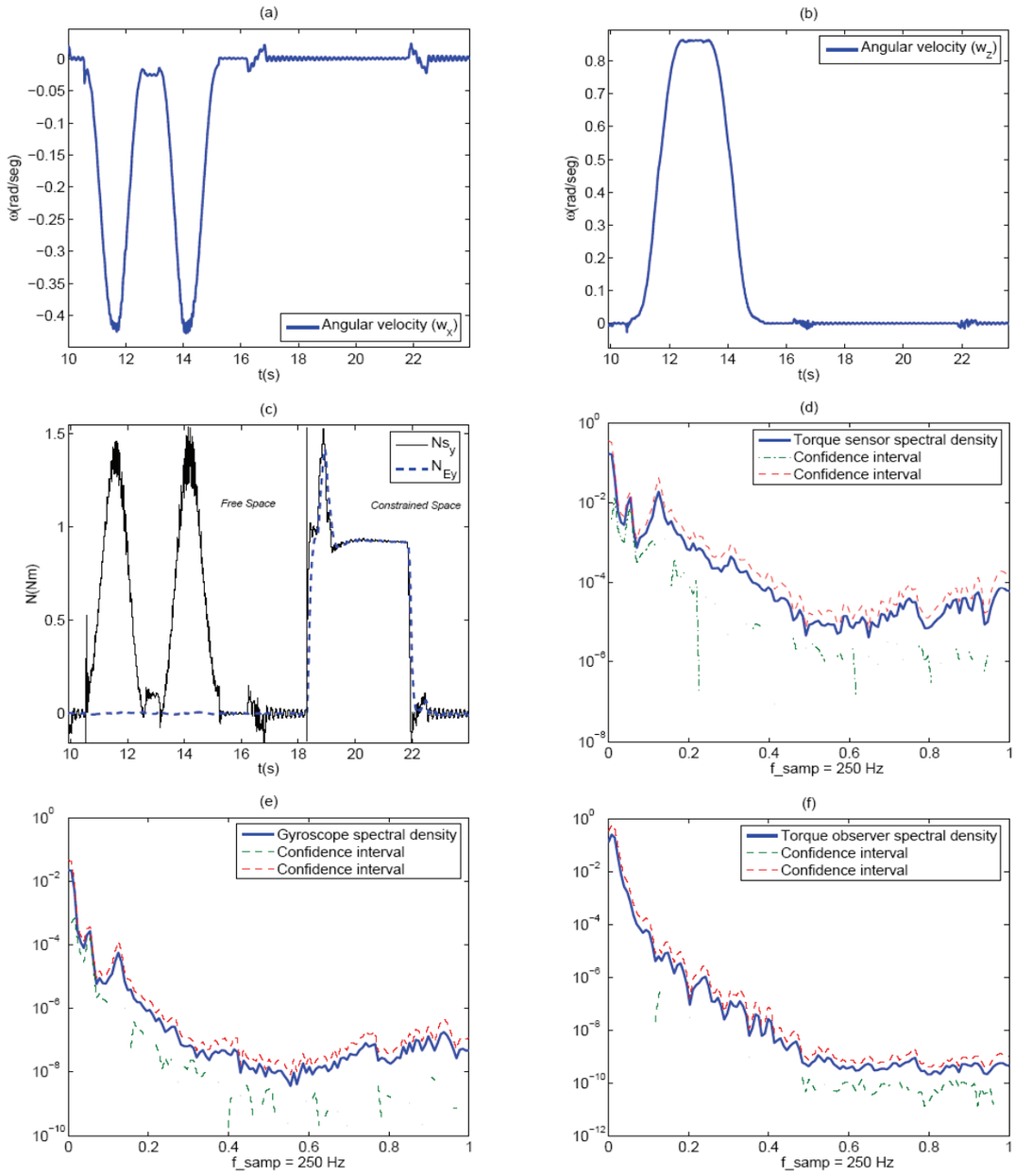

Figure 10. (a) Angular velocity w_x measured with the gyroscope. (b) Angular velocity w_z measured with the gyroscope. (c) Comparison between the torque sensor measurement (N_{S_y}) and the contact torque observer (N_{E_y}) for axis y . (d) Power spectrum density of the torque sensor for axis y . (e) Power spectrum density of the gyroscope sensor for axis x . (f) Power spectrum density of the contact torque observer for axis y . The sampling frequency is 250 Hz

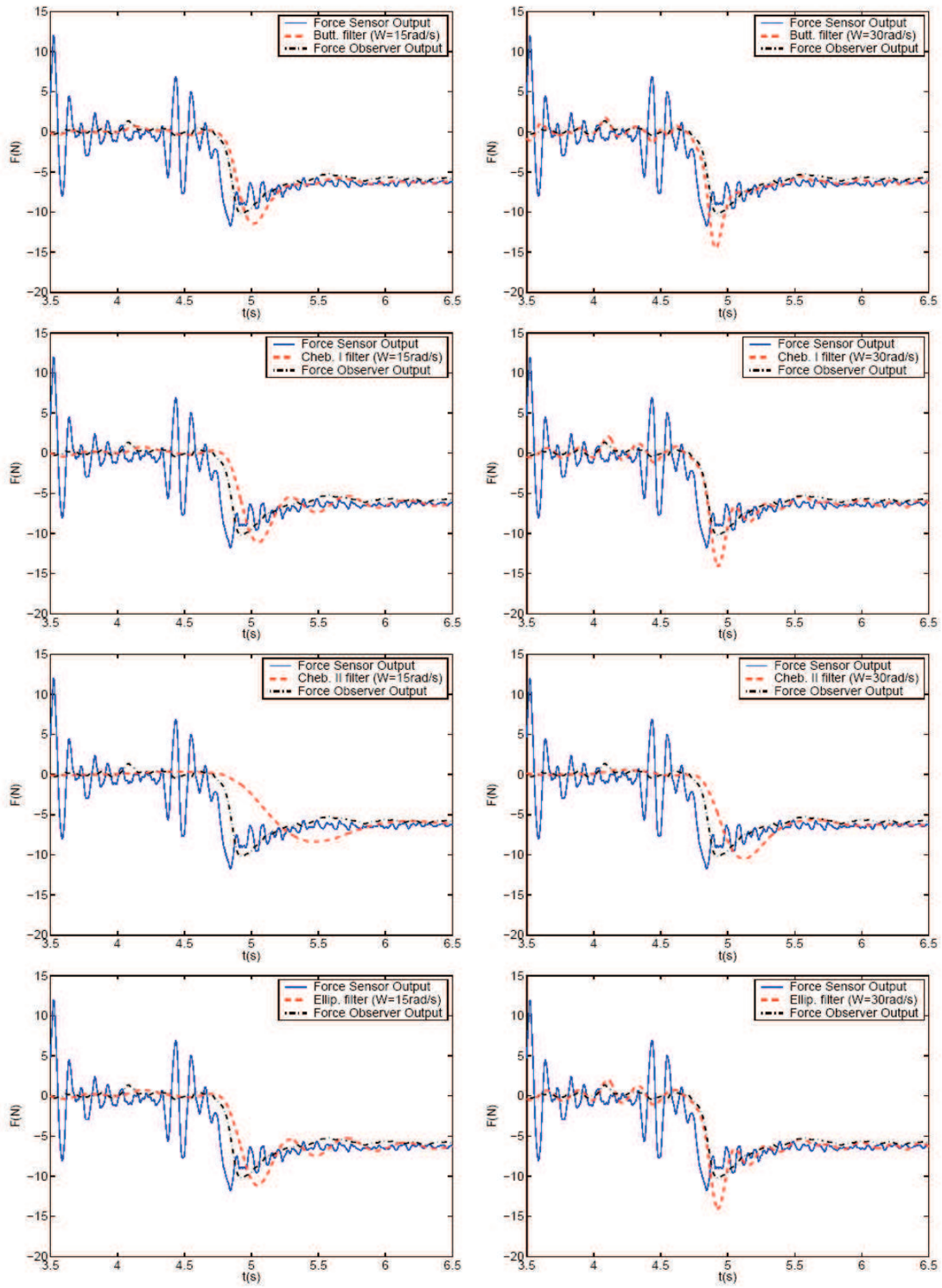

Figure 11. Comparison between the force sensor measurements, the observer outputs and different low-pass filters with different cut-off frequencies (ABB system)

Fig. 11 shows a comparison between the force sensor measurements, the observer output and different low-pass filters with different cut-off frequencies. These figures show results from different configurations of the filters (degree and cut-off frequency) applied to the ABB platform. Analyzing the data, this solution presents two main drawbacks against the proposed contact force observer: depending on the cut-off frequency of the low-filter, they introduce a quite considerable delay; another problem is that these filters also suffers from an overshoot problem.
Finally, another strategy is that before considering the idea of placing an accelerometer at the robot tool to measure its acceleration and, using this measurement to compensate for the inertial forces, the tool acceleration was estimated through the joint measurements and the kinematics robot model (Gamez, 2006a).

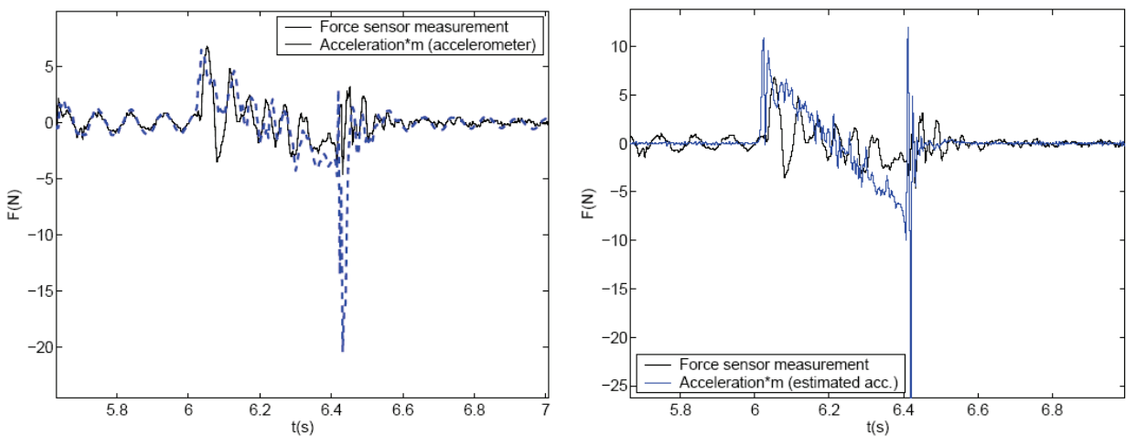

Figure 12. Comparison between the force sensor measurement with the accelerometer output multiplied by the tool mass (upper) and the acceleration estimate using the kinematic model multiply by the tool mass (lower). These experiments were carried out in the Stäubli platform

Figs. 12 show a comparison between the force sensor measurement and the accelerometer output (left), and a comparison between the force sensor signal and the accelerometer estimate (right) for the Stäubli platform. The picture on the left depict how the acceleration measurement follows accurately the force sensor measurement divided by the tool mass. However, it can be appreciated that high accuracy can not be expected because the acceleration estimate, independently from the acceleration estimation algorithm used, does not represent accurately the true acceleration (right).

5. Conclusions

A new contact force observer approach, that fusions the data from three different kind of sensors-that is, resolvers/encoders mounted at each joint of the robot with six degrees of freedom, a wrist force sensor and accelerometers-with the goal of obtaining a suitable contact force estimator has been developed.
We have shown all the advantages and drawbacks of the new sensor fusion approach, comparing the performance of the proposed observers to other alternatives such as the use of the kinematic robot model to estimate the tool acceleration or the use of standard low pass filters.

From the experimental results, it can be concluded that the final observer approach helps to improve the performance as well as stability and robustness for the impact transition phase since it eliminates the perturbations introduced by the inertial forces.
The observer obtained has been validated on several industrial robots applying two well known and widely used control approaches: an impedance control and a hybrid position-force control.
Several successful experiments were performed to validate the performance of the proposed architecture, with a particular interest in compliant motion control. These experiments showed the actual possibility to easily test advanced control algorithms and to integrate new sensors in the developed benchmark as it is the case of the accelerometer.

6. References

Blomdell, A., Bolmsjö, G., Brogårdh, T., Cederberg, P., Isaksson, M. Johansson, R., Haage, M., Nilsson, K., Olsson, M., Olsson, T,. Robertsson, A. and Wang, J.J. (2005). Extending an Industrial Robot Controller---Implementation and Applications of a Fast Open Sensor Interface. *IEEE Robotics and Automation Magazine*, 12(3):85-94. (Blomdell et al., 2005)

Chiaverini, S. , Siciliano, B. and Villani, L. (1999). A Survey of Robot Interaction Control Schemes with Experimental Comparison. *IEEE Trans. Mechatronics*, 4(3):273-285. (Chiaverini et al., 1999)

Gamez, J., Gomez Ortega, J., Gil, M. and Rubio, F. R. (2003). Arquitectura abierta basada en un robot Stäubli RX60 (In Spanish). *Jornadas de Automatica*, pages CD-ROM. (Gamez et al., 2003)

Gamez, J., Robertsson, A., Gomez, J. and Johansson, R. (2004). Sensor Fusion of Force and Acceleration for Robot Force Control. *Int. Conf. Intelligent Robots and Systems (IROS 2004)*, pages 3009-3014, Sendai, Japan. (Gamez et al., 2004)

Gamez, J., Robertsson, A., Gomez, J. and Johansson, R. (2005). Automatic Calibration Procedure for a Robotic Manipulator Force Observer. *IEEE Int. Conf. on Robotics and Automation (ICRA2005)*, pages 2714-2719, Barcelona, Spain. (Gamez et al., 2005a)

Gamez, J., Robertsson, A., Gomez, J. and Johansson, R. (2005). Force and Acceleration Sensor Fusion for Compliant Robot Motion Control. *IEEE Int. Conf. on Robotics and Automation (ICRA2005)*, pages 2720-2725, Barcelona, Spain. (Gamez et al., 2005b)

Gamez, J. (2006). *Sensor Fusion of Force, Acceleration and Position for Compliant Robot Motion Control*. Phd Thesis, Jaen University, Spain. (Gamez, 2006a)

Gamez, J., Robertsson, A., Gomez, J. and Johansson, R. (2006). Generalized Contact Force Estimator for a Robot Manipulator. *IEEE Int. Conf. on Robotics and Automation (ICRA2006)*, pages 4019-4025, Orlando, Florida. (Gamez et al., 2006b)

Gamez, J., Robertsson, A., Gomez, J. and Johansson, R. (2007) Design and Validation of an Open Architecture for an Industrial Robot Control. *IEEE International Symposium on Industrial Electronics (IEEE ISIE 2007)*, pages 2004-2009, Vigo, Spain. (Gamez et al., 2007a)

Gamez, J., Robertsson, A., Gomez, J. and Johansson, R. (2007). Estimación de la Fuerza de Contacto para el control de robots manipuladores con movimientos restringidos (In Spanish). *Revista Iberoamericana de Automática e Informática Industrial*, 4(1):70-82. (Gamez et al., 2007b)

Gamez, J., Robertsson, A., Gomez, J. and Johansson, R. (2008). Self-Calibrated Robotic Manipulator Force Observer (In press). *Robotics and Computer Integrated Manufacturing*. (Gamez et al., 2008a)

Gamez, J., Robertsson, A., Gomez, J. and Johansson, R. (2008). Sensor Fusion for Compliant Robot Motion Control. *IEEE Trans. on Robotics*, 24(2):430-441. (Gamez et al., 2008b)

Grewal, M. S. and Andrews, A. P. (1993). *Kalman Filtering. Theory and Practice*. Prentice Hall, New Jersey, USA. (Grewal and Andrews, 1993)

Harashima, F. and Dote, Y. (1990). Sensor Based Robot Systems. *Proc. IEEE Int. Workshop Intelligent Motion Control*, pages 10-19, Istanbul, Turkey. (Harashima and Dote, 1990)

Hogan, N. (1985). Impedance control: An approach to manipulation, Parts 1-3. *J. of Dynamic Systems, Measurement and Control. ASME*, 107:1-24,. (Hogan, 1985)

IFR. (2001). World Robotics 2001, statistics, analysis and forecasts. *United Nations and Int. Federation of Robotics.* (IFR, 2001)

Jazwinski, A.H. (1970). *Stochastic Processes and Filtering Theory*. Academic Press, New York. (Jazwinski, 1970)

Johansson, R. (1993). *System Modeling and Identification*. Prentice Hall, Englewood Cliffs, NJ. (Johansson, 1993)

Johansson, R. and Robertsson (2003), A. Robotic Force Control using Observer-based Strict Positive Real Impedance Control. *IEEE Proc. Int. Conf. Robotics and Automation*, pages 3686-3691, Taipei, Taiwan. (Johansson and Robertsson, 2003)

Khatib, O. (1987). A unified approach for motion and force control of robot manipulators: The operational space formulation. *IEEE J. of Robotics and Automation*, 3(1):43-53. (Khatib, 1987)

Kröger, T., Kubus, D. and Wahl, F.M. (2006). 6D Force and Acceleration Sensor Fusion for Compliant Manipulation Control. *Int. Conf. Intelligent Robots and Systems (IROS 2006)*, pages 2626-2631, Beijing, China. (Kröguer et al., 2006)

Kröger, T. , Kubus, D. and Wahl, F.M. (2007). Force and acceleration sensor fusion for compliant manipulation control in 6 degrees of freedom. *Advanced Robotics*, 21:1603-1616(14), October. (Kröguer et al., 2007)

Kumar, M., Garg, D. (2004). Sensor Based Estimation and Control of Forces and Moments in Multiple Cooperative Robots. *Trans. ASME J. of Dynamic Systems, Measurement and Control*, 126(2):276-283. (Kumar and Garg, 2004)

Lin, S.T. (1997). Force Sensing Using Kalman Filtering Techniques for Robot Compliant Motion Control. *J. of Intelligent and Robotics Systems*, 135:1-16. (Lin, 1997)

Murray, R. M., Li, Z. and Sastry S.S., A Mathematical Introduction to Robotic Manipulation, *CRC Press*, Boca Raton, FL, 1994. (Murray et al, 1994)

Nilsson, K. and Johansson, R. (1999). Integrated architecture for industrial robot programming and control. *J. Robotics and Autonomous Systems*, 29:205-226. (Nilsson and Johansson, 1999)

Wind River (2005). *VxWorks: Reference Manual*. Wind River Systems. (Wind River, 2005)

Uchiyama, M. (1979). A Study of Computer Control Motion of a Mechanical Arm (2nd report, Control of Coordinate Motion utilizing a Mathematical Model of the Arm). *Bulletin of JSME*, pages 1648-1656. (Uchiyama, 1979)

Uchiyama, M. and Kitagaki, K. (1989). Dynamic Force Sensing for High Speed Robot Manipulation Using Kalman Filtering Techniques. *Proc. of Conf. Decision and Control*, pages 2147-2152, Tampa, Florida. (Uchiyama and Kitagaki, 1989)

Whitney, D. (1985). A Historical Perspective of Force Control. *Proc. IEEE Int. Conf. Robotics and Automation*, pages 262 - 268. (Whitney, 1985)

Robot Manipulators

Edited by Marco Ceccarelli

ISBN 978-953-7619-06-0

Hard cover, 546 pages

Publisher InTech

Published online 01, September, 2008

Published in print edition September, 2008

In this book we have grouped contributions in 28 chapters from several authors all around the world on the several aspects and challenges of research and applications of robots with the aim to show the recent advances and problems that still need to be considered for future improvements of robot success in worldwide frames. Each chapter addresses a specific area of modeling, design, and application of robots but with an eye to give an integrated view of what make a robot a unique modern system for many different uses and future potential applications. Main attention has been focused on design issues as thought challenging for improving capabilities and further possibilities of robots for new and old applications, as seen from today technologies and research programs. Thus, great attention has been addressed to control aspects that are strongly evolving also as function of the improvements in robot modeling, sensors, servo-power systems, and informatics. But even other aspects are considered as of fundamental challenge both in design and use of robots with improved performance and capabilities, like for example kinematic design, dynamics, vision integration.

InTech Europe

University Campus STeP Ri
Slavka Krautzeka 83/A
51000 Rijeka, Croatia
Phone: +385 (51) 770 447
Fax: +385 (51) 686 166
www.intechopen.com

InTech China

Unit 405, Office Block, Hotel Equatorial Shanghai
No.65, Yan An Road (West), Shanghai, 200040, China
中国上海市延安西路65号上海国际贵都大饭店办公楼405单元
Phone: +86-21-62489820
Fax: +86-21-62489821

IntechOpen